

# INSTRUMENTED SINGLE AND GROUP PILES IN BELFAST SOFT CLAY

B.M. Lehane<sup>1</sup>  
B.A. McCabe<sup>2</sup>  
D.T. Phillips<sup>2</sup>

<sup>1</sup> Academic Visitor to Department of Civil and Resource Engineering, University of Western Australia

<sup>2</sup> Research student, Trinity College, Dublin, Ireland

## ABSTRACT

The paper presents a number of key findings from an experimental pile research programme, which is currently underway at a soft clay test bed site on the outskirts of Belfast, Northern Ireland. These findings provide additional insights into the characteristics of driven piles and are used to highlight some inadequacies of standard design procedures for single piles and small pile groups.

## 1 INTRODUCTION

Data recorded by carefully instrumented piles in the field over the past twenty years have greatly advanced our understanding of pile behaviour and have been central to the development of more reliable design methods (e.g. Jardine & Chow 1996 for single driven piles in clay and sand). The success of such field tests recently prompted a relatively comprehensive driven pile testing programme at a soft clay site in Kinnegar, which lies on the shores of Belfast Lough in Northern Ireland. Full descriptions of the experimental work performed to date, which has included combined lateral and axial loading of single piles and both static and cyclic tests on pile groups, is provided in the PhD theses of McCabe (2000) and Phillips (2001). Attention is focussed here on the following three specific aspects of driven pile performance and design:

- (i) The stiffness and capacity of driven piles in small pile groups
- (ii) The effect of an axial pile load on the lateral response of a single driven pile
- (iii) The use of CPT data to assess the ultimate shaft capacity of a single driven pile

These topics are discussed following an initial overview of the soil properties at the test site.

## 2 SOIL PROFILE AND PROPERTIES

Boreholes and piezocone tests revealed a site stratigraphy beneath a 0.7m thick fill layer comprising  $\approx 1.3$ m of alluvial sands, silts and clays overlying  $\approx 7$ m of soft, high plasticity, sensitive clay (referred to locally as 'sleech'). The *sleech* is underlain by a medium dense sand layer at about 9m depth and the water table is  $1.0 \pm 0.2$ m below the ground surface.

### 2.1 UPPER ALLUVIUM

Laboratory tests on this stratum are not presently available but have recently been programmed in the light of their relevance to the interpretation of the lateral load tests discussed in Section 4. The piezocone data indicate it to be a variable combination of layers of firm silty clay and medium dense silty sand. Clay bands comprise two thirds of the stratum and have a typical CPT  $q_t$  value of  $\approx 800$ kPa, which is about four times higher than that of the underlying *sleech*. The sand lenses are medium dense with a mean  $q_t$  value of 2.5MPa.

### 2.2 SOFT CLAY ('SLEECH')

The *sleech* is an estuarine, very lightly overconsolidated, sensitive, plastic clay. The clay fraction ( $\approx 15$ -30%) comprises a mixture of quartz with some illite, chlorite and smectite, while the silt and (small) sand fractions are composed of quartz with  $\approx 15\%$  dolomite and  $\approx 7\%$  calcite. The plasticity and liquidity indices remain constant at about  $35 \pm 5\%$  and 0.8 respectively below a depth of 3.5m. The *sleech* tends to have a lower plasticity and higher silt content at shallower depths.

The overconsolidation ratio (OCR), assessed from oedometer tests on piston samples, reduces from about 1.5 at 2m to close to unity at 9m. These tests indicated maximum compression indices ( $C_c$ ) varying from 0.35 in the siltier material at shallow depth to about 0.75 below 3.5m. The material's behaviour in shear is summarised by one of a number of typical triaxial test results shown on Figure 1. This figure plots the stress path and secant shear stiffness for a piston sample from 4.5m which was subjected to undrained triaxial compression (at an axial strain rate of 5%/day) following anisotropic

consolidation and swelling to OCR=1.5. The dilatant, non-brittle response at this level of overconsolidation as well as the high mobilised friction angle of 30° are unusual for a plastic sensitive clay. The shear stiffness of this sample (Figure 1b) is, however, compatible with a medium to high plasticity clay (e.g. see Smith 1992).

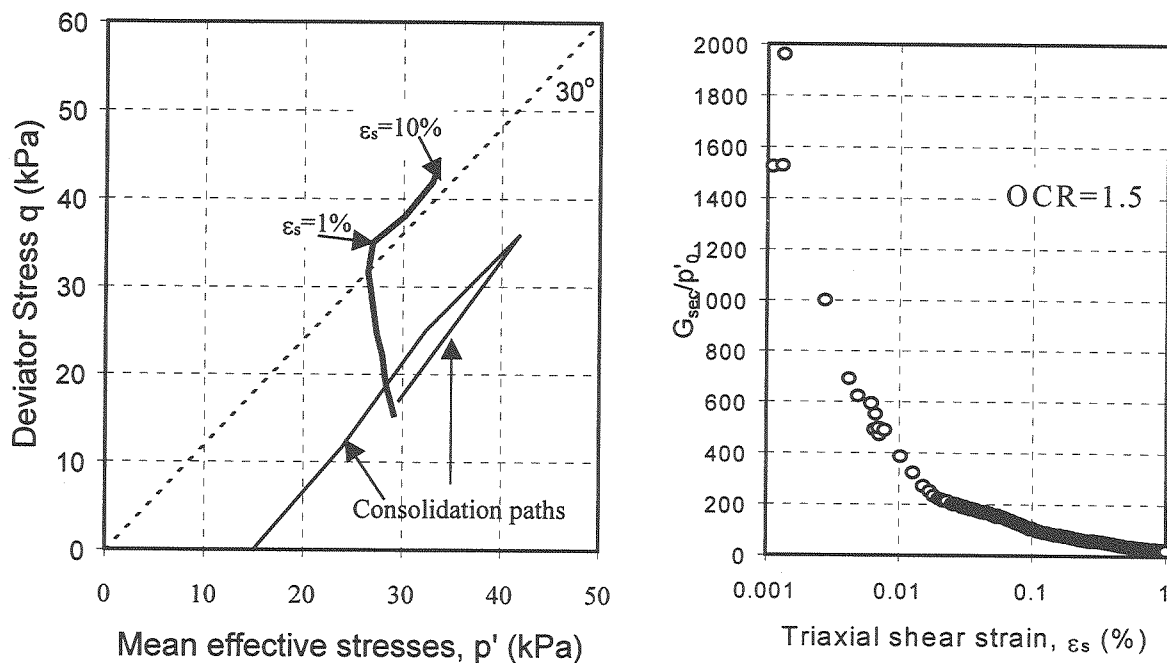


Figure 1 Response of *sleech* piston sample in undrained triaxial compression at OCR=1.5

The more familiar contractant and brittle response of a soft clay, when in a lightly overconsolidated state, was observed in simple shear tests on the material, where high peak friction angles of about 30° were also mobilised. Ring shear tests on reconstituted *sleech* confirmed the existence of low strength clay minerals within the deposit by indicating residual angles of 22 ± 2° and 18 ± 1° for material with clay fractions of 10% and in excess of 20% respectively. These relatively low residual angles have particular relevance to the development of pile shaft friction, which is discussed in Section 5.

### 3 THE STIFFNESS AND CAPACITY OF PILE GROUPS

#### 3.1 TESTING PROGRAMME

Two pile groups, each comprising five 250mm square precast concrete piles were driven to 6m depth and had the plan configuration shown on the inset to Figure 4. The centre to edge pile spacing to pile width ratio ( $s/B$ ) was  $\approx 2.5$ , which is marginally lower than that typically used in practice. ‘Centre’ piles were driven first and were subsequently re-tapped following driving of the edge piles. The time taken to complete driving was less than 2 hours for both groups. The first group was tested in tension using the set-up shown on Figure 2. The second group was tested in compression and employed kentledge to supply the reaction force. Single isolated ‘reference’ piles were also driven to 6m depth and tested in tension and compression so that the pile groups’ response to load could be compared with that of single piles. All piles were tested after full equalisation, which took about 4 months for the pile groups.

Load cells were fixed to anchors embedded in each pile head and were subsequently welded to a pre-fabricated steel pile cap. The pile cap contained two 10mm thick steel plates in between which two levels of 150mm high I-beams ran orthogonally to each other (see Figure 2). The tension load was applied by pulling two high strength bars that were bolted to plates located on the underside of the pile cap. The two jacks were seated on a deep reaction beam and the compressive supports to the applied tension load were provided by slip-coated compression piles that were driven to the sand layer at 9m depth and linked with a concrete cap. The supports for the reaction beam for the compression test were also founded on

slip-coated piles driven to the sand layer so that the load from the kentledge prior to the start of the test did not impose stresses on the clay in the vicinity of the test piles.

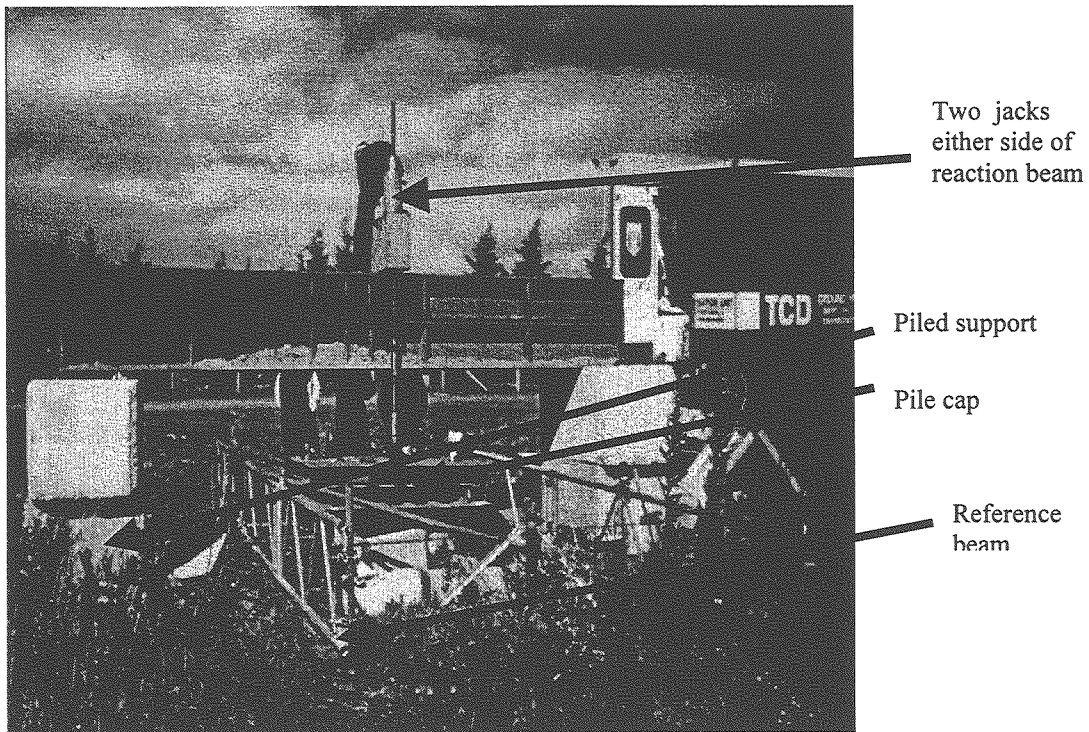


Figure 2 Load test set-up for tension test on pile group

The instrumentation employed in the compression pile group included pressure cells on the centre pile to measure horizontal stresses and both electrical resistance and vibrating wire gauges on the reinforcing steel of all piles to allow measurement of axial load distributions. No instrumentation other than the pile head load cells was employed in the tension pile group, although this group was surrounded by push-in pneumatic piezometers installed at various radial distances and depths. Axial load distributions were also measured in all the single reference pile tests.

### 3.2 INSTALLATION AND EQUALISATION DATA

The data recorded by the instrumentation during pile installation and equalisation are discussed in McCabe (2000) who compares these data with those measured by instrumented 102mm diameter displacement piles installed in a very similar lightly overconsolidated clay at Bothkennar, Scotland (Lehane & Jardine 1994). Observations relevant to stiffness and capacity of the centre pile of the group are provided in McCabe (2000) and are summarised in the following and by Figure 3. This figure plots the variation with time of the horizontal total stresses ( $\sigma_h$ ) acting at a depth of 5.25m on the centre pile of the compression group. These stresses are expressed in the form of the stress ratio,  $H$ , defined as  $H = (\sigma_h - u_0) / \sigma'_{v0}$ , where  $u_0$  and  $\sigma'_{v0}$  are the free field hydrostatic pore pressure and vertical effective stress respectively. The value of  $H$  prior to pile installation is equivalent to  $K_0$  and is the same as the equalised stress ratio,  $K_c$  (defined in Table 1), when full equalisation of stresses following installation is complete.

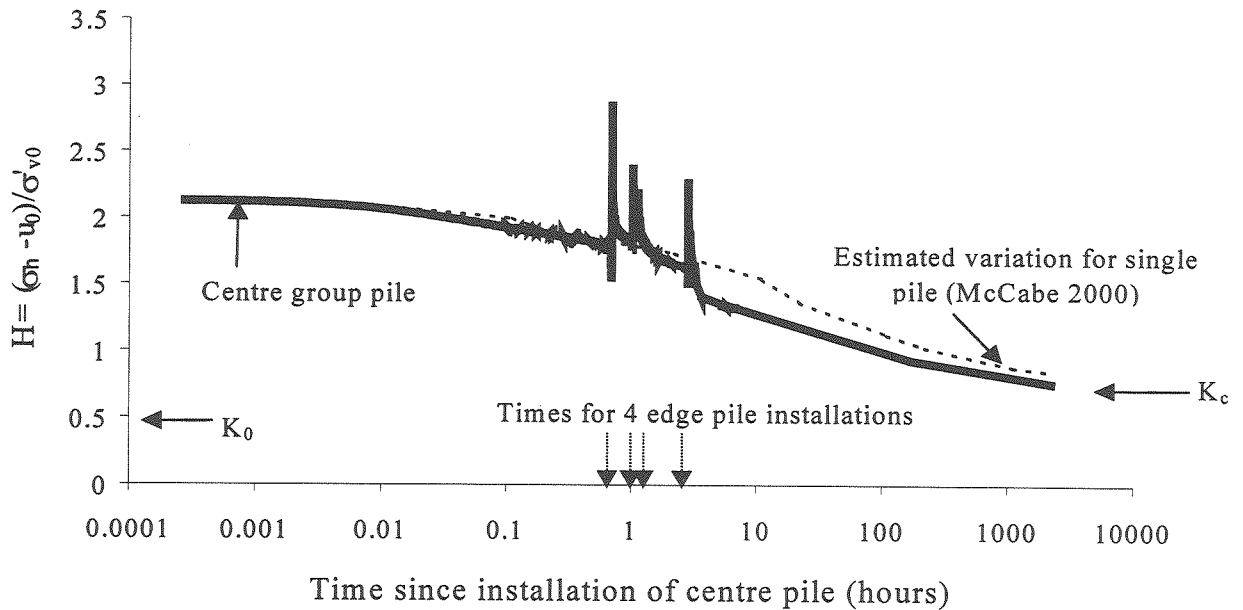


Figure 3 Development on normalised horizontal stress on centre pile in group

Points to note include:

- H measured on the centre pile immediately after its installation is typical of that seen for displacement piles in very lightly overconsolidated clays; see Lehane et al. (1994).
- Subsequent driving of an edge pile leads to an initial slight drop and then a relatively large increase in H on the centre pile. McCabe (2000) shows that the magnitude of the increases are similar to the pore pressure increases generated at the centre pile location by installation of an edge pile in virgin clay.
- The increases in H on the centre pile due to edge pile installation are short-lived and typically reduce to a value close to that existing prior to the driving of an edge pile within a few minutes.
- H values for the centre pile immediately after all four edge piles were driven are about 10 to 20% lower than those recorded after its initial installation.
- Horizontal stresses and pore pressures reduce throughout equalisation as horizontal effective stresses increase. H values for the centre pile continue to lie below those expected for a single pile throughout the equalisation period.

These observations suggest that the shaft capacity of the centre pile of the groups employed is likely to be  $\approx 15\%$  less than that of a single isolated pile. It would appear that the action of installing the edge piles causes destructuration of the clay (in addition to that caused by driving the centre pile) and a further reduction in effective stresses of the clay in the vicinity of the centre pile.

### 3.3 LOAD TEST DATA

The tests were load controlled and allowed creep rates to fall below  $\approx 0.24\text{mm/hour}$  before application of the next load increment. Displacement measurements made throughout the tests indicated that the pile cap behaved in a fully flexible manner during the tension group test (all piles took the same load), but was effectively rigid during the compression group test (all piles moved by the same amount). The flexible response in tension occurred partly because of the difficulty in achieving an adequate weld between the I-beams in the cap.

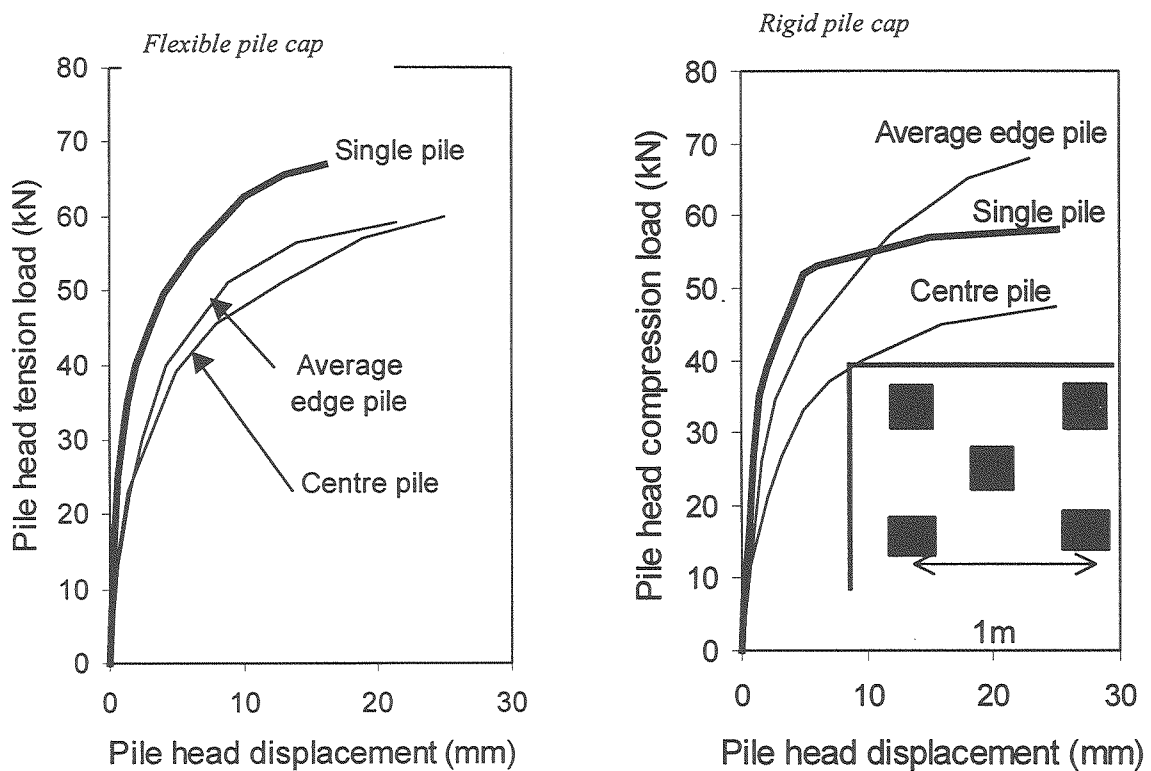


Figure 4 Load displacement data recorded in single pile and pile group tests

The observed load-displacement data of the centre and edge piles in tension and compression are plotted on Figure 4. This figure also shows the responses of the single reference piles to tension and compression loading. It is evident that:

- (i) The reference tension pile had a larger ultimate capacity than that of the compression reference pile even though both were tested after the same equalisation period. Further tests at the site have shown that this arises partly because the soil in the vicinity of the piles tested in compression, which was  $\approx 20\text{m}$  distant from the other piles, was of a slightly lower consistency.
- (ii) The ultimate capacities of the centre pile in both the compression and tension pile groups are about 20% less than the ultimate capacities of the corresponding reference piles. This shortfall in capacity is compatible with the trends shown by the horizontal stresses on Figure 3.
- (iii) Interaction effects lead to a much softer load-displacement response of group piles than those of the single piles. Interaction in the compression group is more significant because of the rigidity of the pile cap for this case.
- (iv) Although the trend is not clear for all cases, the stiffness and ultimate capacity of the edge piles fall somewhere between those of a single pile and the centre group pile.

On the basis of these observations, it may be surmised that the ultimate capacity of group piles in soft clay for  $s/B \geq 3$  (i.e. slightly larger than the  $s/B$  value in the experiments) can be taken to be about the same as that of a single pile. The stiffness of group piles installed at such a spacing is, however, likely to be less than half of that of a single pile.

### 3.4 PREDICTION OF GROUP PILE RESPONSES

The response of the group piles during the load tests is now compared with that predicted using the PIGLET computer program (Randolph 1983), which is typical of the type of pile group programs used worldwide in standard design. This program assumes that the soil is a linear elastic continuum and assesses interaction factors between piles using the expressions developed in Randolph and Wroth (1979). The group analyses adopted a constant soil shear modulus ( $G$ ) with depth of 4000kPa and employed a rigid pile cap for the compression test and a flexible cap for the tension test. The  $G$  value was selected to give a relatively accurate prediction of the load-displacement relationship of the single reference piles up to  $\approx 50\%$  of their ultimate capacities and equates to the  $G_{sec}$  value at a triaxial shear strain of  $\approx 0.07\%$  and a  $G_{sec}/c_u$  value of 200 (see Figure 1b).

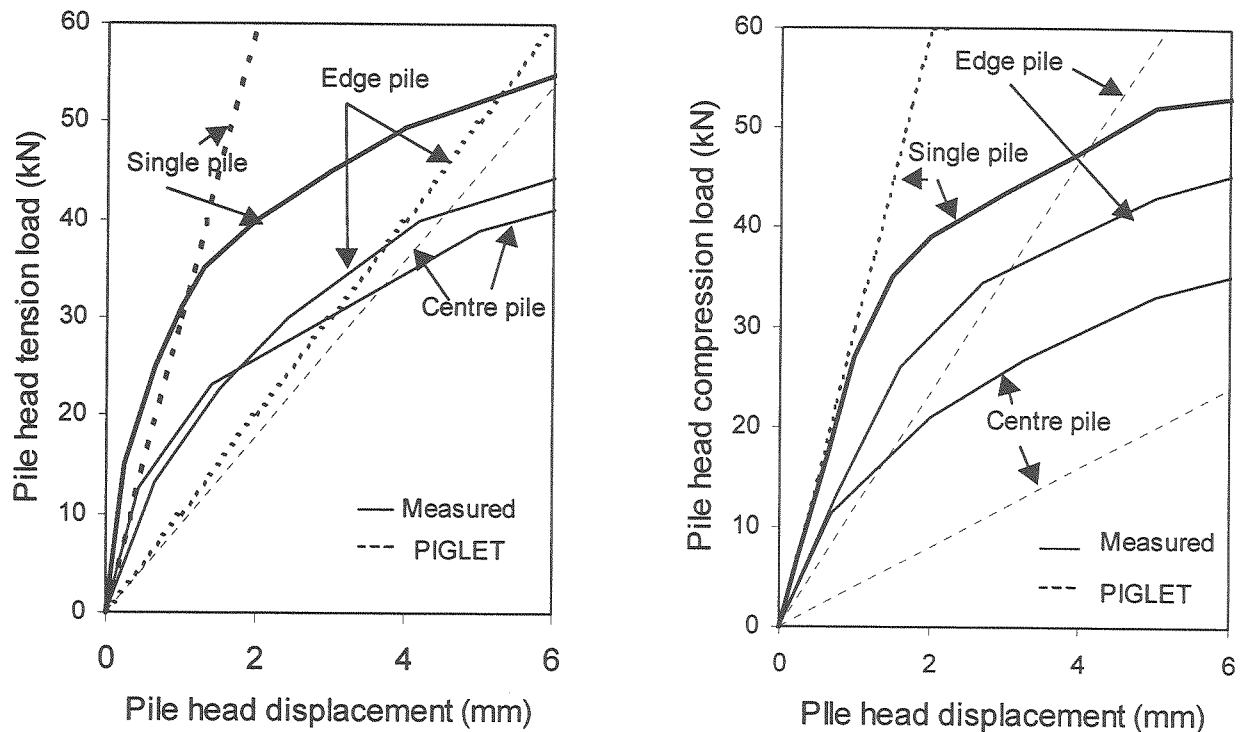


Figure 5 Single and group pile response at low displacements

The predictions for the compression and tension tests are compared on Figure 5 with the observed responses for pile head displacements up to 6mm. The inadequacies of the linear elastic soil model employed are self-evident. Interaction between piles, particularly for the case with the rigid pile cap, are over-estimated significantly and may well be over-estimated by an even greater margin for larger pile groups. However, the great difficulties associated with the prediction of installation effects means that designers do not have reliable alternative methods of analysis for groups comprising displacement piles at their disposal. On the evidence of the tests described, designers can continue (and are likely to do so for some time to come) to use programs such as PIGLET to obtain a very conservative estimate of driven pile group stiffness.

#### 4 THE EFFECT OF AN AXIAL PILE LOAD ON LATERAL PILE RESPONSE

##### 4.1 EXPERIMENTAL DETAILS

Two 350mm square instrumented precast concrete piles, designated *L1* and *AL1*, were driven, 2m apart, into the sand layer at 9m. Both piles had centrally placed inclinometer tubes, each of which housed a string of electro-levels for monitoring pile displacement profiles. They also contained strategically located pressure cells in addition to electrical and vibrating strain gauges on the piles' reinforcing bars.

The soil in front of each pile was removed to a depth of 0.7m to reduce the effect of the stiffer near surface fill material on the lateral pile response. An axial load of 460kN was then applied to pile *AL1* while leaving pile *L1* with no vertical load (although this pile had a residual axial load at its base of 125kN due to negative skin friction). The axial load of 460kN, which was equivalent to the total weight of the loading frame and kentledge employed, induced a pile head settlement of 2.6mm and was maintained while subjecting both *AL1* and *L1* to a maximum lateral load of 60kN one day after applying the vertical load. Lateral load tests to failure were conducted on the following day and also one year later.

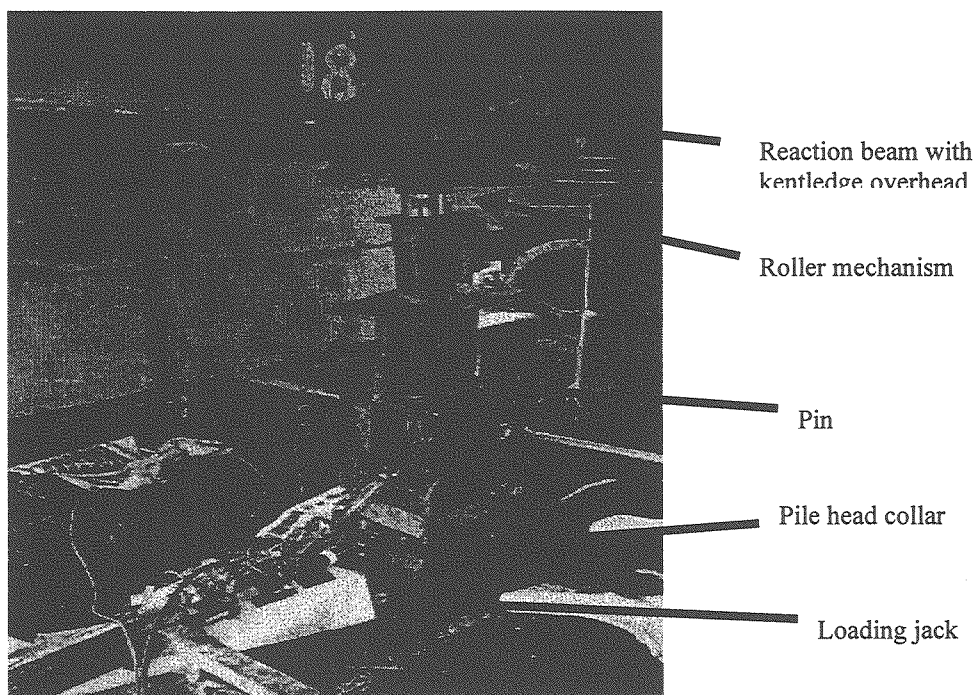


Figure 6 Photo of pile head mechanism at failure in Pile AL1

The mechanism used to load the head of pile AL1 is shown on Figure 6 and included rollers at the underside of the beam supporting the kentledge and a pin just above the pile collar. The system was designed to permit free rotation and lateral displacement at the pile head while allowing the vertical load to be carried centrally on the pile. However, strain gauge measurements made above ground level indicated that friction had caused the application of a small (righting) moment to the pile head. It was fortunate that the instrumentation allowed this moment to be measured reliably, and allowed for when interpreting the test results.

#### 4.2 LATERAL LOAD TEST RESULTS

The lateral load displacement ( $F_h$ - $\delta$ ) curves measured during the first lateral tests on piles AL1 and L1 are shown on Figure 7. It is clear that there is a dramatic difference between the piles' responses, with pile AL1 moving 4mm under a lateral load of 60kN while pile L1 moves 24mm under the same lateral load. Moreover, pile L1 indicates a distinctly non-linear characteristic and, on unloading, experiences a permanent lateral displacement of 7.5mm. The recovery of pile AL1 is large, verifying the more elastic response of this pile.

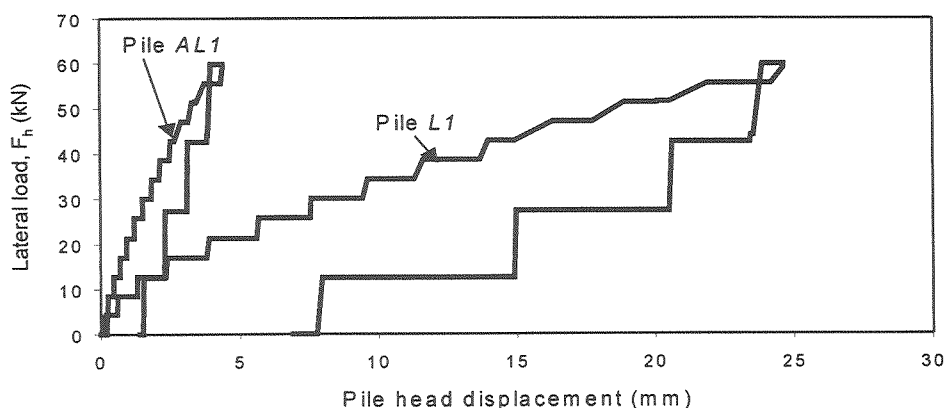


Figure 7 Lateral load-displacement response measured on first time loading of piles L1 and AL1

Non-linear finite element analyses of the pile sections combined with on-site calibrations allowed the pile bending moments to be deduced from the strain gauge data with confidence. These moments and the displacement profiles derived from the electro-level data are plotted on Figures 8 and 9 respectively for four levels of applied lateral load. It is evident that lateral movements are concentrated in the upper 2m of the soil stratum and that the lateral response of the piles is controlled by the properties of the stiff alluvium overlying the *sleech*. Maximum bending moments occur at a depth of about 2m and, for these tests, just fall short of the moment at which cracking of the concrete is initiated. The non-zero moment at the top of pile *AL1* is a consequence of the friction in the mechanism at the head of this pile.

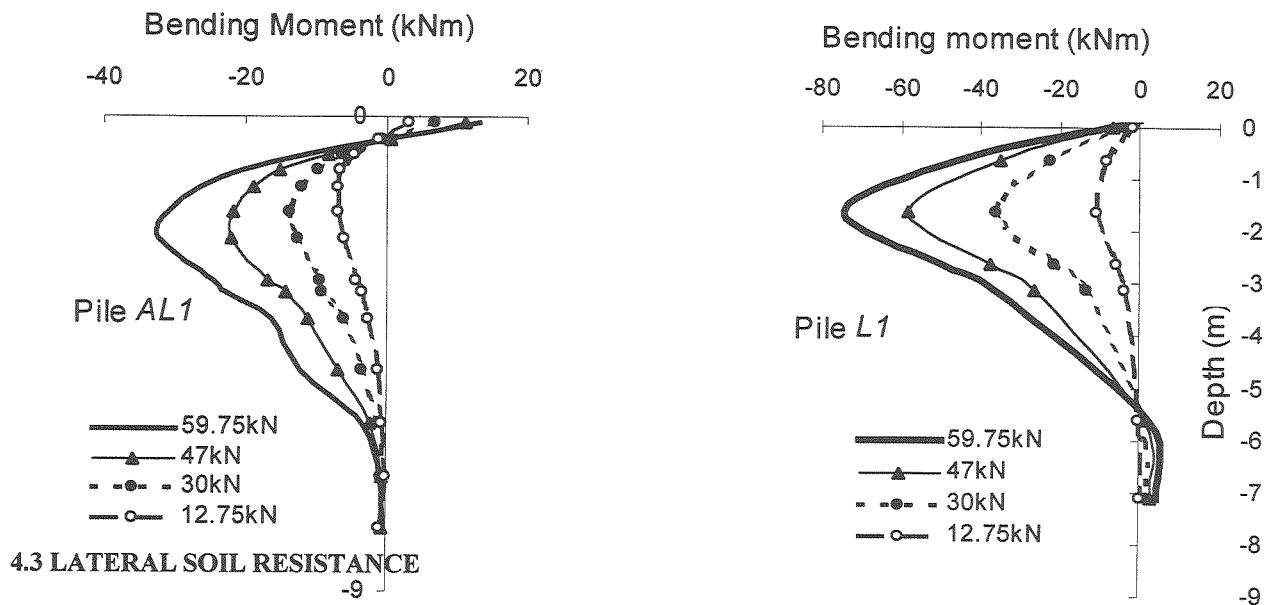


Figure 8 Bending moments deduced from strain gauge data on piles *AL1* and *L1*

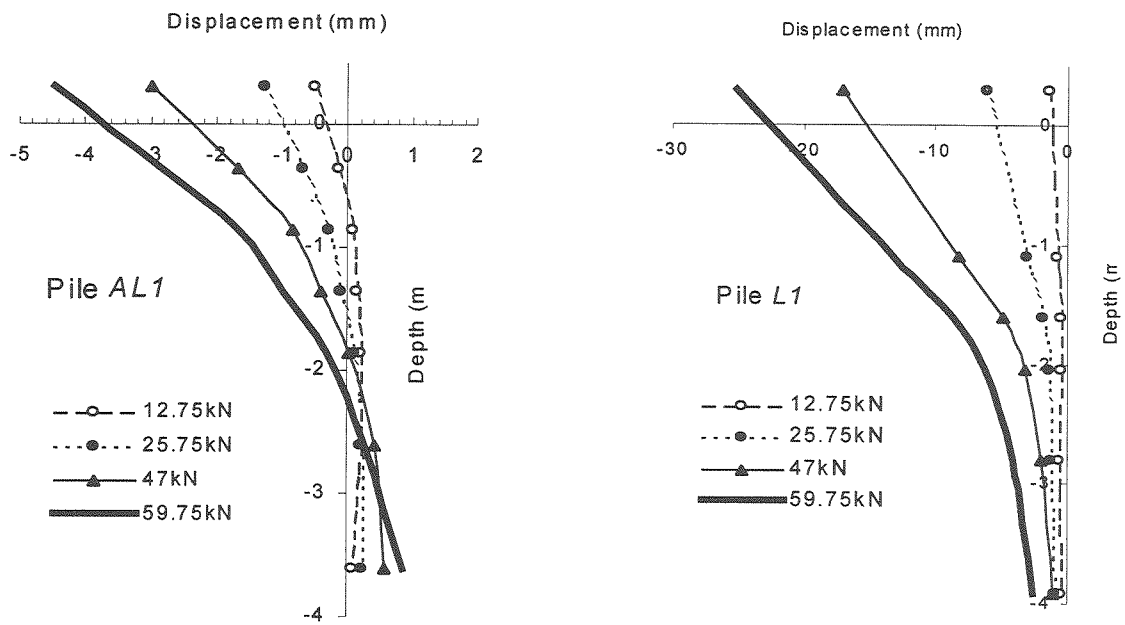


Figure 9 Displacement profiles deduced from electro-levels on piles *AL1* and *L1*

4.3 LATERAL SOIL RESISTANCE

Net soil forces per unit length ( $p$ ) inducing the bending moments on Figure 8 can be derived by double differentiation of the moment profile. Simple numerical differentiation of the moments measured at the typical strain gauge spacing of 0.25m would lead to gross errors in the  $p$  values evaluated in this manner. It was therefore necessary to derive best-fit differentiable expressions for each set of moment-depth profiles. The following general algebraic form for the moment ( $M$ ) at any distance below the level of the applied lateral load ( $z$ ) was found to be most successful for this purpose:

$$M(z) = [1 - 1/(e^{-a_0 z} + 1)] [ a_1 + a_2 z + a_3 z^2 + a_4 z^3 + \dots + a_i z^{i-1} ] \tag{1a}$$

where the constants  $a_i$  ( $i=0,n$ ) were selected to provide the best fit to a given measured moment-depth profile. The shear, given as  $F=dM/dz$ , at  $z=0$  is equal to the value of the applied lateral load ( $F_h$ ) and the reaction ( $p=d^2M/dz^2$ ) at  $z=0$  is equal to zero. These constraints imply:

$$a_1 = -2 M(z=0) \tag{1b}$$

$$a_2 = 2 F_h + a_0 a_1 / 2 \tag{1c}$$

$$a_3 = a_0 a_2 / 2 \tag{1d}$$

Values of  $p$  were derived in this way for all load increments applied to piles  $L1$  and  $AL1$ . The pile displacement data combined with these  $p$  values yield the  $p$ - $y$  or load transfer curves for the soil. Those curves obtained within the alluvium are presented in Figure 10 in terms of the net soil pressure ( $P$ ) against normalised displacement ( $y/B$ ), which is a direct scaling by  $B$  of the  $p$ - $y$  form.

The curves derived for the alluvium adjacent to pile  $L1$  are compatible with the API recommendations for firm clay (API 1993), assuming an ultimate lateral capacity ( $P_u$ ) of 200kPa and the  $E50$  strain parameter of 0.01 suggested for firm clay. This  $P_u$  value was estimated by extrapolating the curves on Figure 10a and equates to about 4.5 times the anticipated average undrained strength of the material (of 45kPa). The factor of 4.5 is reasonable in view of the fact that a pit to a depth of 0.7m was excavated in front of the pile (e.g. see Randolph and Houlsby 1984).

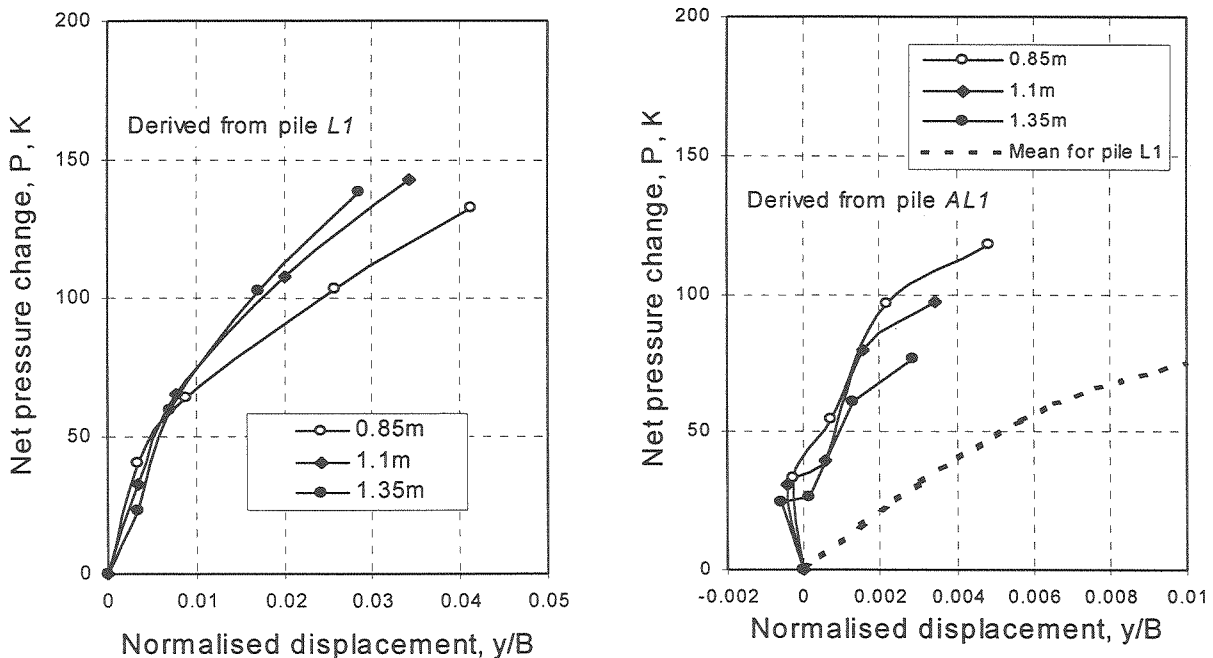


Figure 10 Derived lateral resistance at three levels within the alluvium

The P-y/B response of the alluvium next to pile ALI is, however, three to four times stiffer than that next to pile LI. The initial negative displacements seen in the curves derived from pile ALI on Figure 10b (and also Figure 9) are a consequence of the small applied moment to this pile, which evidently has affected the derived response. Both piles were loaded laterally a year later with no applied axial load and pile ALI actually showed a softer response than pile LI on this occasion. Differences observed on Figure 10 cannot therefore be attributed to variability of the alluvium

One possible explanation for these differences is that the axial load on pile ALI (which increased the skin friction in this material from a downdrag shear stress of  $\approx 10\text{kPa}$  to a positive shear stress of  $20\text{ kPa}$ ) led to an increase in horizontal effective stress and hence to an increase in lateral soil stiffness. Preliminary numerical analyses indicate that such increases can only be explained if the alluvium is strongly dilatant (Phillips 2001). The most likely explanation is that the assumption of non-interacting springs implicit in the derivation of the  $p-y$  or P-y/B curves is in error and that the derivation of any set of load transfer curves depends significantly on the pile displacement profile induced by the applied loads and moments. Recent studies by Ashour & Norris (2000), who predict the response of passive strain wedges adjacent to laterally loaded piles, support this explanation and suggest that the moment that was (inadvertently) applied to pile ALI led to the differences observed. Designers therefore need to be aware that  $p-y$  curves are not independent of the pile loading conditions.

### 5 SHAFT CAPACITY OF SINGLE DRIVEN PILES FROM CPT DATA

Peak local shaft shear stresses ( $\tau_f$ ) inferred from load distribution curves measured in a tension test on a 250mm square concrete pile driven to 6m are shown on Figure 11a. These are compared with  $\tau_f$  values recorded in a load test on a 102mm diameter steel pile jacked to the same depth in soft clay at Bothkennar, Scotland (Lehane & Jardine 1994). The clay at Bothkennar is also slightly overconsolidated and, as shown on Figure 11b, has a similar consistency (as indicated by the CPT  $q_t$  profiles) to that at Belfast between depths of 2m and 6m.

The comparable modes of penetration of driven piles and cone penetrometers has prompted the development of many empirical formulae relating  $q_t$  and shaft friction. One of the most popular in use is the simple relationship proposed by Bustamante & Gianeselli (1982) which gives:

$$\tau_f = q_c / \beta \approx q_t / \beta \tag{2}$$

where the value of  $\beta$  recommended for driven piles in soft clay with  $q_t < 1\text{MPa}$  is 30. Application of this correlation to the  $q_t$  profiles on Figures 11 implies average shaft shear stresses between 3m and 6m at Kinnegar and Bothkennar of 8.5kPa and 10.7kPa respectively. The measured average values of 12kPa at Kinnegar and 20kPa at Bothkennar are higher than these predictions. More significantly, however, the relative difference in capacities is evidently much larger than that of the  $q_t$  values, implying that the magnitude of  $\beta$  varies with the nature of the soft clay deposit.

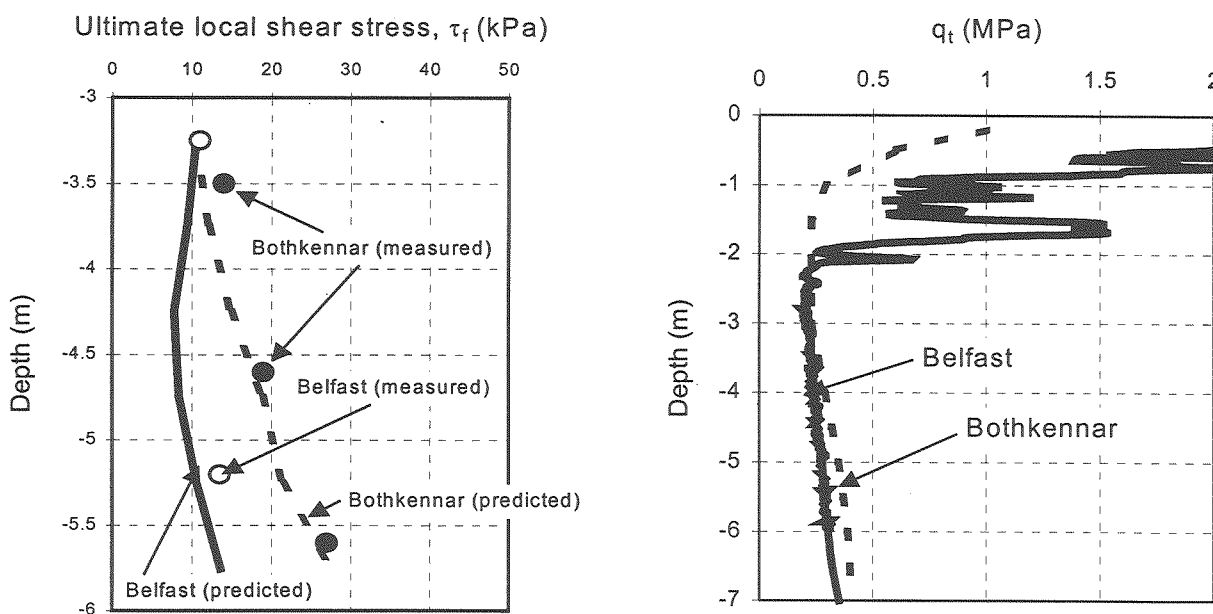


Figure 11 (a) Predicted and measured ultimate shear stresses (b)  $q_t$  profiles in Belfast and Bothkennar sites

Lehane et al. (2000) recently proposed a CPT-based approach for driven piles in clay. This approach builds upon the effective stress methods proposed by Lehane et al. (1994) and Jardine & Chow (1996) by employing the CPT  $q_t$  value rather than the clay's overconsolidation ratio (OCR) as a measure of clay consistency. The method, which is summarised on Table 1, applies the simple Coulomb friction relationship to derive  $\tau_f$  and incorporates observed characteristics of displacement piles such as:

- 1 the dependence of the horizontal stresses acting on the pile shaft after equalisation on the relative depth of the pile tip ( $h$ ), the clay's sensitivity and the consistency of the clay as described by the  $q_t$  value.
- 2 the formation of a residual shear surface at the interface between the pile shaft and clay; the operational interface friction for use in Coulomb's friction relationship is equivalent to that measured in appropriate ring shear interface tests.

All data required for the calculations of  $\tau_f$  using this approach are provided in Lehane and Jardine (1994) and McCabe (2000) and are summarised in Table 2. The predicted  $\tau_f$  profiles are plotted on Figure 11a and are seen provide a good match to the magnitudes and distributions of the measurements. Notably, the approach also predicts the relative difference between the  $\tau_f$  values recorded at the sites. The calculations in Table 2 indicate that the primary reason for this difference is the low  $\delta_f$  value of  $18^\circ$  in the Belfast *sleech* compared to the higher interface residual friction angle of  $31^\circ$  for Bothkennar clay. This example therefore serves to highlight the inadequacy of expressions such as equation (2) and the importance of measuring residual interface friction angles for displacement pile design. Ramsey et al. (1998) provide a detailed specification on how appropriate angles can be measured, at relatively low cost, using the ring shear apparatus.

## 6 CONCLUSIONS

The driven pile experiments at the soft clay test site have shown:

- 1 The ultimate shaft capacity of a group pile in soft clay with  $s/B \approx 2.5$  is about 80% of that of a single isolated pile while its stiffness is less than half of that of a single pile. Pile group models which presume linear elastic soil behaviour under-predict group pile stiffness significantly.
- 2 The API recommendations for the  $p$ - $y$  curves of the alluvium at the test site are reasonable when an axial pile load is absent, but they under-predict the lateral soil stiffness by a factor of four when an axial pile load and restricting pile head moment are present.
- 3 Predictions for pile shaft capacity require an assessment of the soil's residual interface friction angle.

## 7 ACKNOWLEDGEMENTS

The authors would like to gratefully acknowledge the support provided by the UK Institution of Civil Engineers (London), Lowry Piling (Dublin), John Barnett & Assoc. (Dublin) and Imperial College (London). The first author would also like to acknowledge the support provided by the Gledden Fellowship for his sabbatical leave at UWA, which facilitated the production of this paper and its presentation to the AGS, Perth.

## 8 REFERENCES

- API (1993). RP2A: Recommended practice of planning, designing and constructing fixed offshore platforms. 19<sup>th</sup> edition, Washington, American Petroleum Institute, USA.
- Ashour, M. and Norris G. (2000). Modeling lateral soil-pile response based on soil-pile interaction. *J. Geotech. and Env. Engng.*, 126(5), 420-428.
- Burland, J.B. (1990). On the compressibility and shear strength of natural clays. *Geotechnique*, 40(3), 327-378.
- Bustamante M. and Gianceselli L. (1982). Pile bearing capacity prediction by means of static penetrometer CPT. *Proc. 2<sup>nd</sup> European Symp. On Penetration Testing*, Amsterdam, 2, 493-500.
- Jardine R.J. and Chow F.C. (1996). *New Design Methods for Offshore Piles*. MTD publication 96/103, HSE Books, London.
- Lehane, B.M. and Jardine, R.J. (1994). Displacement pile behaviour in a soft marine clay. *Canadian Geotech. J.*, 31(2), 181-191.
- Lehane, B.M., Jardine R.J., Bond A.J. and Chow F.C. (1994). The development of shaft resistance on displacement piles in clay. *Proc. 13<sup>th</sup> Int. Conf. Soil Mech. and Foundation Engng.*, New Delhi, 2, 473-476.
- Lehane, B.M., Chow F.C., McCabe B.A. and Jardine R.J. (2000). Investigating potential relationships between the shaft capacity of closed-ended piles driven in clay and the CPT end resistance. *Geotech. Engng.*, 143, 93-101.
- McCabe B.A. (2000). The behaviour of driven pile groups in soft clay. PhD Thesis, Univ. of Dublin (Trinity College).

- Phillips D.M. (2001). Field studies of the lateral behaviour of driven piles in soft and stiff clay. PhD Thesis, Univ. of Dublin (Trinity College).
- Ramsey N., Jardine R.J., Lehane B.M. and Ridley A. (1998). A review of soil-steel interface testing with the ring shear apparatus. *Proc. Conf. On Offshore Site Investigation and Foundation Behaviour*, Society for Underwater Technology, London, Kluwer, 237-258.
- Randolph, M.F. (1983). PIGLET users manual. Int. Report, Cambridge Civil Engineering Dept., UK.
- Randolph M.F. and Wroth C.P. (1979). An analysis of the vertical deformation of pile groups. *Geotechnique*, 29(4), 423-439.
- Randolph, M.F. and Houlsby, G.T. (1984). The limiting pressure on a circular pile loaded laterally in cohesive soil. *Geotechnique*, 34(4), 613-623.
- Smith, P.R. (1992). Properties of high compressibility clays with reference to construction on soft ground. PhD thesis, Univ. of London (Imperial College).

**Table 1.** Evaluation of  $\tau_f$  using Lehane et al. (2000)

$\tau_f$	= $f_L K_c \sigma'_{v0} \tan \delta_f$
$K_c$	= $\sigma'_{rc} / \sigma'_{v0}$
where	
$\tau_f$	= Peak local shaft shear stress
$f_L$	= Load coefficient, normally assumed=0.8
$\sigma'_{rc}$	= Equalised radial/horizontal effective stress
$\sigma'_{v0}$	= Free field vertical effective stress
$\delta_f$	= Angle of interface friction
$\delta_f$ depends on many factors but can be assessed from ring shear experiments that model (a) the properties of the pile surface, (b) the displacement and rate history and (c) the normal effective stress level.	
$K_c$ is evaluated as:	
$K_c$	= $[(q_t / \sigma'_{v0})^{0.6} (h/R)^{-0.2}] (0.3 + 0.3e^{-I_{vr}})$ for $I_p \geq 35\%$
	= $[(q_t / \sigma'_{v0})^{0.6} (h/R)^{-0.2}] (0.45 + 0.15e^{-I_{vr}})$ for $I_p < 35\%$
where	
$q_t$	= CPT $q_c$ value with pore pressure correction
$h/R$	= Distance from the pile tip normalised by the equivalent pile radius
$I_{vr}$	= Relative void index
$I_p$	= Plasticity index
$I_{vr}$ is a measure of the clay sensitivity and overconsolidation ratio and is defined as:	
$I_{vr}$	= $(e_0 - e_{ICL}) / C_c^*$ , where
$e_0$	= In situ void ratio
$e_{ICL}$	= Void ratio of the reconstituted material at $\sigma'_v = \sigma'_{v0}$
$C_c^*$	= Slope of the virgin consolidation line of the reconstituted material in $(e, \log_{10} \sigma'_v)$ space
$e_{ICL}$ , $e_{100}^*$ and $C_c^*$ can be derived from standard index test results using relationships proposed by Burland (1990):	
$e_{ICL}^*$	= $e_{100}^* - C_c^* \log_{10}(\sigma'_{v0}/100)$ , $\sigma'_{v0}$ in kPa
$e_{100}^*$	= $0.109 + 0.679 e_L - 0.089 e_L^2 + 0.016 e_L^3$
$C_c^*$	= $0.256 e_L - 0.04$

**Table 2.** Calculation of  $\tau_f$  at Belfast and Bothkennar using Lehane et al. (2000)

<i>Kinnegar</i> (Soils data reported in McCabe 2000)											
Depth	$\sigma'_{v0}$	$q_t$ (kPa)	$h/R$	w	LL	$I_p$ (%)	e	$e_L$	$I_{vr}$	$\tan \delta_f$	$\tau_f$ (kPa)
3.25	34.5	220	19.5	0.48	0.58	30	1.30	1.566	0.315	0.40	10.5
3.75	37.5	240	16.0	0.5	0.675	36	1.35	1.823	0.048	0.31	9.4
4.25	40.5	250	12.4	0.67	0.75	42	1.81	2.025	0.772	0.31	7.8
4.75	43.5	260	8.9	0.67	0.72	42	1.81	1.944	0.947	0.31	8.4
5.25	46.5	290	5.3	0.64	0.72	40	1.73	1.944	0.799	0.31	10.6
5.75	49.5	295	1.8	0.64	0.72	40	1.73	1.944	0.826	0.31	13.6
<i>Bothkennar</i> (Soils data reported in Lehane & Jardine 1994)											
Depth	$\sigma'_{v0}$	$q_t$ (kPa)	$h/R$	w	LL	$I_p$ (%)	e	$e_L$	$I_{vr}$	$\tan \delta_f$	$\tau_f$ (kPa)
3.25	33.6	250	54.1	0.58	0.61	35	1.57	1.647	0.859	0.60	10.3
3.75	36.6	290	44.3	0.61	0.65	35	1.65	1.755	0.868	0.60	12.1
4.25	39.9	315	34.4	0.65	0.75	35	1.76	2.025	0.653	0.60	14.9
4.75	42.5	340	24.6	0.65	0.82	50	1.76	2.214	0.398	0.60	18.9
5.25	45.2	360	14.8	0.66	0.82	50	1.78	2.214	0.476	0.60	21.4
5.75	48.5	385	4.9	0.67	0.82	50	1.81	2.214	0.558	0.60	27.7